AMERICAN SOCIETY FOR MICROBIOLOGY | Journal of Bacteriology®

RESEARCH ARTICLE

Disruption of a Novel Iron Transport System Reverses Oxidative Stress Phenotypes of a *dpr* Mutant Strain of *Streptococcus mutans*

Tridib Ganguly,[a] Jessica K. Kajfasz,[a] James H. Miller,[b] Eric Rabinowitz,[a] Lívia C. C. Galvão,[b,c*] Pedro L. Rosalen,[c] Jacqueline Abranches,[a] José A. Lemos[a]

[a]Department of Oral Biology, University of Florida College of Dentistry, Gainesville, Florida, USA

[b]Center for Oral Biology, University of Rochester Medical Center, Rochester, New York, USA

[c]Department of Physiological Sciences, Piracicaba Dentistry School, University of Campinas, Piracicaba, SP, Brazil

ABSTRACT The Dps-like peroxide resistance protein (Dpr) is essential for H_2O_2 stress tolerance and aerobic growth of the oral pathogen *Streptococcus mutans*. Dpr accumulates during oxidative stress, protecting the cell by sequestering iron ions and thereby preventing the generation of toxic hydroxyl radicals that result from the interaction of iron with H_2O_2. Previously, we reported that the SpxA1 and SpxA2 regulators positively regulate expression of *dpr* in *S. mutans*. Using an antibody raised against *S. mutans* Dpr, we confirmed at the protein level the central and cooperative nature of SpxA1 and SpxA2 regulation in Dpr production. During phenotypic characterization of the *S. mutans* Δ*dpr* strain, we observed the appearance of distinct colony variants, which sometimes lost the oxidative stress sensitivity typical of Δ*dpr* strains. Whole-genome sequencing of these phenotypically distinct Δ*dpr* isolates revealed that a putative iron transporter operon, *smu995-smu998*, was a genomic hot spot with multiple single nucleotide polymorphisms identified within the different isolates. Deletion of *smu995* or the entire *smu995-smu998* operon in the Δ*dpr* background strain completely reversed the oxidative stress-sensitive phenotypes associated with *dpr* inactivation. Conversely, inactivation of genes encoding the ferrous iron transport system FeoABC did not alleviate phenotypes of the Δ*dpr* strain. Preliminary characterization of strains lacking *smu995-smu998*, *feoABC*, and the iron/manganese transporter gene *sloABC* revealed the interactive nature of these three systems in iron transport but also indicated that there may be additional iron uptake systems in *S. mutans*.

IMPORTANCE The dental caries-associated pathogen *Streptococcus mutans* routinely encounters oxidative stress within the human plaque biofilm. Previous studies revealed that the iron-binding protein Dpr confers protection toward oxidative stress by limiting free iron availability, which is associated with the generation of toxic hydroxyl radicals. Here, we report the identification of spontaneously occurring mutations within Δ*dpr* strains. Several of those mutations were mapped to the operon *smu995-smu998*, revealing a previously uncharacterized system that appears to be important in iron acquisition. Disruption of the *smu995-smu998* operon resulted in reversion of the stress-sensitive phenotype typical of a Δ*dpr* strain. Our data suggest that the Smu995-Smu998 system works along with other known metal transport systems of *S. mutans*, i.e., FeoABC and SloABC, to coordinate iron uptake.

KEYWORDS *Streptococcus*, iron homeostasis, Dpr, oxidative stress

Received 31 January 2018 **Accepted** 30 April 2018

Accepted manuscript posted online 7 May 2018

Citation Ganguly T, Kajfasz JK, Miller JH, Rabinowitz E, Galvão LCC, Rosalen PL, Abranches J, Lemos JA. 2018. Disruption of a novel iron transport system reverses oxidative stress phenotypes of a *dpr* mutant strain of *Streptococcus mutans*. J Bacteriol 200:e00062-18. https://doi.org/10.1128/JB.00062-18.

Editor Olaf Schneewind, University of Chicago

Copyright © 2018 American Society for Microbiology. All Rights Reserved.

Address correspondence to José A. Lemos, jlemos@dental.ufl.edu.

* Present address: Lívia C. C. Galvão, Department of Dentistry, CEUMA University, São Luis, Maranhão, Brazil.

T.G. and J.K.K. contributed equally to this article.

The oral bacterium *Streptococcus mutans* is a major etiological agent associated with dental carries due to its abilities (i) to synthesize large quantities of extracellular polymers of glucan from sucrose that serve as a scaffold for bacterial tooth colonization, (ii) to transport and metabolize a wide range of carbohydrates at low pH values, and (iii) to survive under acidic pH conditions that are lethal to commensal oral bacteria (1, 2). In dental plaque, *S. mutans* must also cope with oxidative stresses that arise from bacterial respiration and from the utilization of oral hygiene products (3). In addition, members of the mitis group of streptococci (e.g., *S. gordonii* and *S. sanguinis*) are net producers of hydrogen peroxide (H_2O_2), and a series of studies have demonstrated an inverse correlation between proportions of *S. mutans* and mitis streptococci in oral health and disease, with high numbers of *S. mutans* bacteria associated with caries and high proportions of mitis streptococci associated with health (4, 5).

Although H_2O_2 is a weak oxidizing agent, it is a neutral molecule that quickly penetrates the bacterial membrane and, in the presence of ferrous iron (Fe^{2+}), takes part in the Fenton reaction, which generates highly reactive hydroxyl radicals. In contrast to the case for H_2O_2, hydroxyl radicals cannot be scavenged by enzymatic reactions and cause irreversible cellular damage by attacking membrane lipids, triggering enzyme mismetallation, or directly targeting proteins and DNA (6). To minimize the deleterious effects of the Fenton reaction, iron uptake in cells is tightly regulated, and any excess of intracellular free iron ions is rapidly immobilized by ubiquitous iron-binding proteins called ferritins (7). In bacteria, ferritin-like proteins are known as Dps (DNA-binding protein from starved cells) or Dpr (Dps-like peroxide resistance), which are functionally similar to but structurally different from mammalian ferritins (8–10). Moreover, some bacterial Dps/Dpr proteins have been shown to bind to DNA, forming a stable complex that further protects the DNA molecule from oxidative damage (11).

In spite of the fact that they do not encode a catalase, streptococci are able to tolerate up to millimolar concentrations of H_2O_2 (2, 3). In several streptococcal species, Dpr was shown to be essential for bacterial tolerance to oxidative stress (12–16). In *S. mutans*, the gene encoding Dpr was initially shown to be essential for aerotolerance, as a *dpr* mutant strain could not grow on agar plates when exposed to air, a phenotype that was fully reversed by the addition of catalase to the growth medium or by anaerobic incubation (14, 17). Recently, we showed that the *dpr* gene of *S. mutans* is positively regulated by the oxidative stress regulators SpxA1 and SpxA2 (18). In a recent study that aimed to characterize novel Spx-regulated genes, we included a *dpr* deletion (Δ*dpr*) strain as a benchmark strain for a number of oxidative stress sensitivity assays (18). In addition to confirming the essentiality of Dpr for aerobic growth and survival in the presence of H_2O_2, this study also revealed that the Δ*dpr* strain was highly sensitive to iron overload and, most importantly, had reduced infectivity in a rat caries model (18). However, during the study, we noticed the appearance of subpopulations of the Δ*dpr* strain that have lost the heightened sensitivity to oxidative stress. Here, we demonstrate that this phenotypic reversion was stable after multiple passages, and whole-genome sequencing (WGS) of these phenotypically reverted *dpr* mutant strains revealed single nucleotide polymorphisms (SNPs) in genes coding for a putative Fe^{3+} ferrichrome ABC transporter (*smu995-smu998* operon). By designing clean deletions in this putative iron transport system, we confirmed that disruption of *smu995-smu998* reverts the extreme sensitivity of the Δ*dpr* strain to oxidative stress. The present work reveals that the Smu995-Smu998 system is a previously uncharacterized transport system involved in iron uptake and provides novel insights into oxidative stress tolerance mechanisms in *S. mutans*. Because homologs of Smu995-Smu998 are found in several other streptococci, the findings described here should have broader implications.

RESULTS AND DISCUSSION

Dpr accumulates during aerobic growth and H_2O_2 stress in an Spx-dependent manner. Previously, Yamamoto and colleagues showed that Dpr accumulated in the *S.*

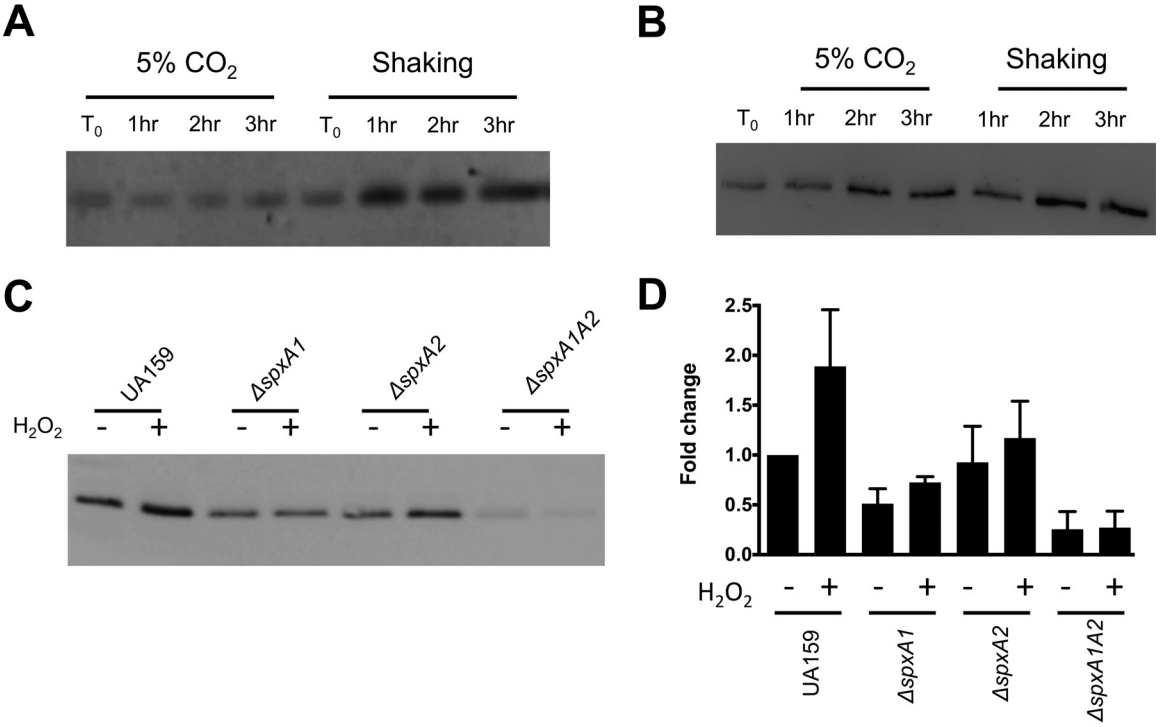

FIG 1 Accumulation of Dpr during oxidative stress. (A and B) *S. mutans* UA159 was grown statically in a 5% CO_2 atmosphere to mid-log phase (OD_{600} of 0.4) and split in two aliquots; one was kept in 5% CO_2 and the other was incubated under vigorous aeration (shaking at 200 rpm). Protein lysates were prepared from samples that were removed hourly, separated by SDS-PAGE, and subjected to Ferene S staining (20 μg protein lysate per well) (A) or Western blot analysis (2 μg protein lysate per well) (B) using anti-*S. mutans* Dpr antibodies. (C) Western blot analysis, using anti-*S. mutans* Dpr antibodies, of lysates from *S. mutans* UA159 Δ*spxA1*, Δ*spxA2*, or Δ*spxA1* Δ*spxA2* cells (2 μg protein lysate per well) that were grown statically in 5% CO_2 to an OD_{600} of 0.4 and then split in two aliquots, one treated with 0.5 mM H_2O_2 (+) and one left untreated (−) for 60 min. (D) Densitometry of the Western blots shown in panel C was performed with Bio-Rad ImageQuant software. Data shown are the averages and standard deviations from three independent experiments.

mutans cytoplasm during aerobic growth (9). The high affinity of Dpr for iron and its status as the primary iron-binding protein of streptococci allow the iron-specific stain Ferene-S to be used as a proxy to determine the iron-binding affinity of Dpr (14). To test the impact of exposure to oxygen upon protein-bound iron levels, the *S. mutans* UA159 and Δ*dpr* strains were grown statically at 37°C in a 5% CO_2 incubator or under aeration (shaking culture at 37°C in a standard incubator) for up to 3 h. When protein cell lysates were separated by gel electrophoresis and stained with Ferene-S, a single band of the predicted size of Dpr (~16 kDa) was detected in the parent strain (Fig. 1A) but not in lysates of the Δ*dpr* strain (data not shown), thereby confirming that the 16-kDa band indeed corresponds to Dpr. The intensity of the staining clearly indicated that more iron molecules were bound to Dpr upon aeration (shaking) than in cells grown statically in 5% CO_2 (Fig. 1A). This result suggests that in response to aeration, the abundance of iron molecules bound to Dpr increases as the cells attempt to reduce the availability of free iron that could potentially participate in Fenton chemistry. Based on previous evidence (9, 18), we expected the increase in iron-bound Dpr to correlate with an increase in total Dpr levels. To confirm this possibility, we generated a polyclonal antibody against Dpr and used it to determine Dpr levels in cells grown under the same conditions used for Fig. 1A. As expected, Dpr accumulated over time in cells grown under shaking conditions (Fig. 1B). However, Dpr also accumulated over time in cells grown in 5% CO_2, indicating either that some level of oxidative stress occurs in the 5% CO_2 atmosphere as the cultures approach stationary phase or that stationary-phase accumulation of Dpr is not oxidative stress dependent. Thus, it appears that the ability of Dpr to sequester iron molecules is enhanced under aeration, supporting data reported when free iron pools were measured before and after aeration in a Δ*dpr* strain of *S. mutans* GS-5 (9). At this time, it is not completely clear if this phenomenon is due

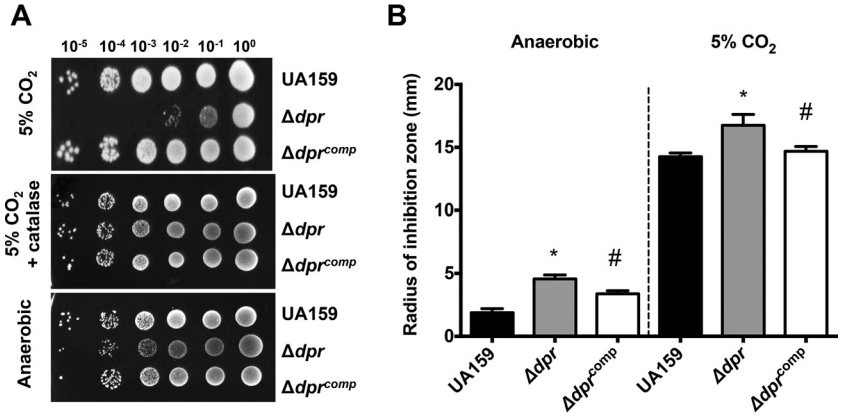

FIG 2 Genetic complementation of the Δ*dpr* strain. (A) *S. mutans* UA159, Δ*dpr*, and Δ*dpr*^{comp} strains were grown anaerobically to mid-log phase, at which point 10-fold serial dilutions of cultures were spotted onto BHI agar plates and incubated in a 5% CO_2 atmosphere in the presence or absence of catalase or anaerobically. (B) Absence of Dpr increases sensitivity to the iron-dependent antibiotic streptonigrin. Early-log-phase cultures of UA159, Δ*dpr*, and Δ*dpr*^{comp} strains grown anaerobically were swabbed on BHI agar plates and then topped with filter paper discs soaked with a streptonigrin solution. Growth inhibition zones were measured after 24 h of incubation at 37°C, either anaerobically or in 5% CO_2. Data shown are the averages and standard deviations for three independent cultures. *, statistical significance compared to UA159 ($P < 0.01$, one-way analysis of variance [ANOVA]); #, indicates statistical significance compared to the Δ*dpr* strain ($P < 0.01$, one-way ANOVA).

to an increase in the intracellular pools of free iron molecules or to an enhanced efficiency of Dpr to sequester iron during aeration. However, the latter seems more likely, as the 1-h time points reveal similar quantities of Dpr protein in lysates incubated under 5% CO_2 or shaking conditions (Fig. 1B), while a notably enhanced potential for iron binding was observed for the shaking cultures (Fig. 1A).

Recently, we showed that transcription of *dpr* is induced by H_2O_2 (peroxide) stress and that this induction was dependent on the activity of the transcriptional regulators SpxA1 and SpxA2 (18). In agreement with this observation, Dpr protein levels nearly doubled in the parent strain after exposure to peroxide stress (Fig. 1C). Compared to the parent strain, the Δ*spxA1*, Δ*spxA2*, and double mutant Δ*spxA1* Δ*spxA2* strains harbored reduced basal levels of Dpr. Furthermore, when cultures of the Δ*spx* strains were treated with H_2O_2, cells lacking SpxA1 but not SpxA2 did not show increased expression of Dpr (Fig. 1C). Notably, production of Dpr was nearly abolished in the Δ*spxA1* Δ*spxA2* double mutant strain (Fig. 1C). These trends fit well with the transcriptional data previously described, pointing to SpxA1 as the major regulator of *dpr* expression in response to oxidative stress, while SpxA2 is responsible for basal levels of expression (18). Thus, while *dpr* may be controlled by other transcriptional factors such as the negative regulator PerR (19), it seems that the bulk of *dpr* transcription relies on the positive transcriptional activation by SpxA1 and SpxA2.

Phenotypes of the Δ*dpr* strain can be rescued by genetic complementation. The importance of the *S. mutans* Dpr in oxidative stress tolerance has been well established, as we and others have shown that inactivation of *dpr* has multiple negative implications for *S. mutans* fitness, including extreme sensitivity to growth in air or in the presence of H_2O_2 (9, 14, 17, 18, 20). As described in greater detail below, the Δ*dpr* strain is phenotypically unstable, a phenomenon first discovered upon observing altered colony morphology of the Δ*dpr* strain struck on agar plates. To ensure that these variants were not the result of unexpected polar effects due to the *dpr* deletion and because none of the previous studies included the genetic and phenotypic complementation of *S. mutans* Δ*dpr* strains, we used the integration vector pMC340B to genetically complement the Δ*dpr* strain. As shown before, the Δ*dpr* strain was extremely sensitive to growth in the presence of air (i.e., 5% CO_2), a phenotype that could be fully rescued by the addition of catalase to the agar plates or by incubating plates under anaerobic conditions (Fig. 2A). Most importantly, genetic complementation of

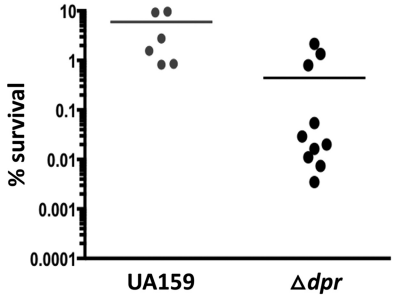

FIG 3 The *S. mutans* Δ*dpr* strain is phenotypically unstable. When exposed to a lethal concentration of $FeSO_4$ (5 mM), independent cultures of the Δ*dpr* strain fall into two phenotypically distinct clusters: one is highly sensitive (~3-log-greater sensitivity than UA159), while the other is moderately sensitive to $FeSO_4$.

Δ*dpr* (Δ*dpr*^{comp} strain) fully restored the ability of the strain to grow in the 5% CO_2 incubator.

Sensitivity to the iron-dependent antibiotic streptonigrin has been used as an indirect approach to estimate free iron content in bacterial cells (21). Enhanced sensitivity to streptonigrin indicates that there is a greater abundance of free iron available for coordination with streptonigrin in the cell. As expected, the Δ*dpr* strain was significantly more sensitive than the parent strain to streptonigrin when incubated under either anaerobic or 5% CO_2 conditions, a phenotype that was also restored in the Δ*dpr*^{comp} strain (Fig. 2B). Therefore, we can conclude that phenotypic reversions of subpopulations of the Δ*dpr* strain are not associated with polar effects.

Identification of phenotypically unstable populations of the Δ*dpr* strain. As mentioned above, during phenotypic characterization of the Δ*dpr* strain, we noticed the appearance of two distinct colony morphologies, either "rough" or "smooth," when the Δ*dpr* strain was struck on agar plates and incubated in a 5% CO_2 atmosphere. This observation prompted us to characterize individual Δ*dpr* colony isolates when we observed a bipartite phenotype in individual isolates exposed to a lethal concentration of $FeSO_4$. Specifically, individual colony isolates of the Δ*dpr* strain fell into one of two groups, such that one group (highly sensitive) showed ~1,000-fold reduction in survival compared to the parent strain, while the other group (moderately sensitive) showed survival rates that were only 10-fold lower than that of the parent strain (Fig. 3). When individual colonies were recovered at the completion of the assay, we found that those Δ*dpr* isolates displaying increased resistance to $FeSO_4$ grew well on plates kept in the CO_2 incubator in the absence of catalase and were much less sensitive to H_2O_2 stress than Δ*dpr* isolates that remained highly sensitive to $FeSO_4$ (data not shown). However, no direct correlation between the colony morphology (i.e., "rough" versus "smooth") and stress sensitivity could be drawn. Importantly, the phenotype reversions of the Δ*dpr* isolates were stable after multiple passages, suggesting that these Δ*dpr* variants harbor mutations that, at least in part, compensate for the loss of Dpr. As a safeguard, we took measures to avoid the emergence of these variations when working with the Δ*dpr* strain. Specifically, we always worked with fresh plates that were streaked from the frozen stock on plates containing catalase and incubated anaerobically. Once these precautions were adopted, we consistently observed the expected behavior of the Δ*dpr* strain, with high sensitivity to $FeSO_4$ and H_2O_2 and no noticeable alterations in colony morphology.

In an attempt to identify a genetic change(s) associated with the phenotypic reversal of a subset of Δ*dpr* isolates, we subjected three Δ*dpr* colonies with different phenotypes to whole-genome sequencing (WGS) analysis: one "smooth" colony that remained stress sensitive (Δ*dpr*-A) and two colonies that had become stress tolerant, one with a "rough" colony phenotype (Δ*dpr*-B) and one with a "smooth" colony phenotype (Δ*dpr*-C). In addition, the lab stock UA159 parent strain was resequenced as a reference to the different Δ*dpr* isolates. Using computational tools (see Materials and

TABLE 1 Spontaneous mutations in Δ*dpr* isolates as determined by whole-genome sequencing

Isolate (phenotype)	Reference nucleotide (UA159)	Variant nucleotide	Reference amino acid (UA159)	Variant amino acid	Gene locus	Proposed function
Δ*dpr*-A mutant (smooth colony, stress sensitive)	T	A	M	K	*smu995*	Iron transport
	A	T			Intergenic region, *smu1378-smu1379*	
	A	T			Intergenic region, *smu1378-smu1379*	
	A	G			Intergenic region, *smu1378-smu1379*	
	T	A			Intergenic region, *smu1378-smu1379*	
	T	G			Intergenic region, *smu1635c-smu1636c*	
Δ*dpr*-B mutant (smooth colony, stress tolerant)	T	A	C	S	*smu995*	Iron transport
	G	A	G	S	*smu995*	Iron transport
	G	T	G	V	*smu995*	Iron transport
Δ*dpr*-C mutant (rough colony, stress tolerant)	G	A	R	Q	*smu257* (*oppC*)	ABC transporter
	G	T			Intergenic region, *smu910-smu911c*	
	C	A	A	D	*smu998*	Iron transport
	C	T	A	T	*smu2091c* (*mutS*)	DNA repair

Methods) that compared the genome sequences of the three Δ*dpr* isolates to that of our UA159 genome, one or more SNPs were identified in each one of the three Δ*dpr* strains (Table 1). Remarkably, all Δ*dpr* variants displayed SNPs within genes of the *smu995-smu998* operon, which is predicted to encode a putative ferric (Fe^{3+}) ferrichrome permease transporter based on BLAST search analysis. The proteins encoded by the *smu995-smu998* operon share approximately 80% similarity to a putative ferrichrome permease present in group B *Streptococcus* (GBS) and in *Streptococcus pneumoniae* but have limited similarities to other putative ferrichrome permeases previously characterized in group A streptococcus (GAS) and GBS (FtsABCD and FhuCDBG, respectively) (Fig. 4) (22, 23).

In the Δ*dpr*-A isolate, a smooth colony that remained stress sensitive, the annotated start codon of *smu995* was changed to a lysine (M→K). Careful observation of the sequence upstream of the putative start codon revealed a second ATG six bases upstream, which was unchanged in the Δ*dpr*-A isolate and may serve as the actual start codon. If this is correct, the SNP that changed the coding sequence from a methionine to a lysine may not have affected Smu995 functionality. Six additional SNPs were identified in the Δ*dpr*-A isolate, although those SNPs were all within noncoding regions.

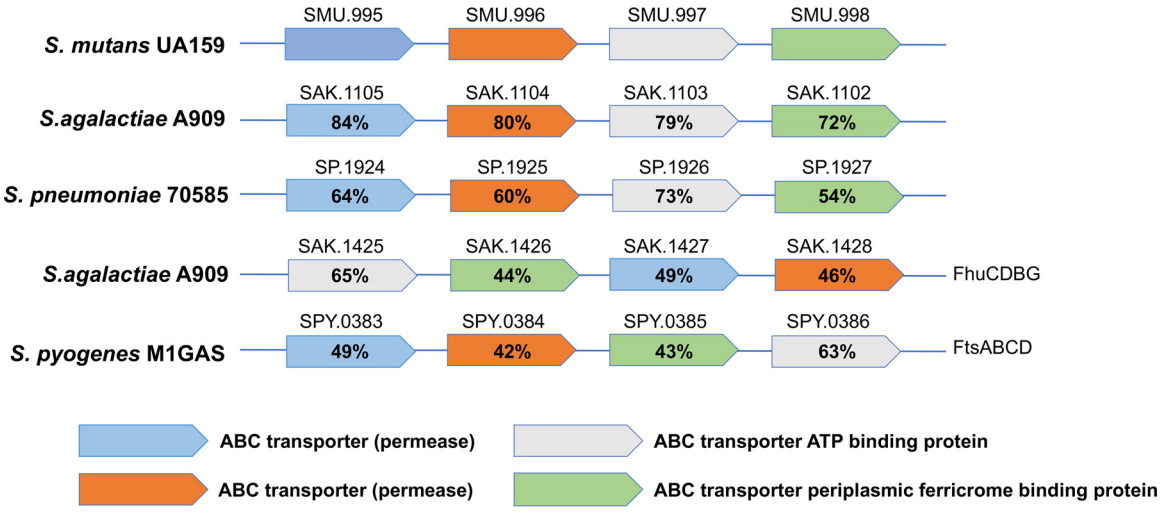

FIG 4 Similarities of the *S. mutans* Smu995-Smu998 proteins and homologs in other streptococci as determined by BLAST analysis. Color-coded boxes represent the organization of the genes within various streptococcal species, while the numeric values indicate the percent similarity at the protein level.

Three SNPs were identified in the Δ*dpr*-B genome (stress-tolerant, rough colony), all within the *smu995* coding region, including a cysteine-to-serine substitution (C→S) at residue 66, a glycine to serine substitution (G→S) at residue 67 and a glycine-to-valine substitution (G→V) also at residue 67. While any one of these amino acid substitutions may have potentially affected Smu995 function, the replacement of the cysteine residue by serine is the most likely to impair protein function given that conserved cysteine residues are critical for the function of iron transport proteins of *Klebsiella pneumoniae* and *Pseudomonas aeruginosa* (24, 25). Finally, four SNPs were identified in the Δ*dpr*-C isolate (stress-tolerant, smooth colony). Though one substitution was in a noncoding region, the additional SNPs were found within coding regions, including one encoding an arginine-to-glutamine (R→Q) substitution within the gene (*smu257*) coding for the transmembrane permease OppC, one encoding an alanine-to-threonine (A→T) substitution within the gene (*smu2091*) coding for the DNA mismatch repair protein MutS, and one encoding an alanine-to-aspartic acid substitution (A→D) within *smu998*, the last gene of the *smu995-smu998* operon. Regardless of whether a particular Δ*dpr* isolate regained oxidative stress tolerance or not, the results from the WGS indicate that the *smu995-smu998* operon is a genetic hot spot in the Δ*dpr* strain.

A clean deletion of *smu995* or of the entire *smu995-smu998* operon alleviates the stress sensitivity of the Δ*dpr* strain. The multiple SNPs identified within the *smu995-smu998* operon in Δ*dpr* variants point to an association between iron uptake by Smu995-Smu998 and Dpr. This association is logical given that in the absence of Dpr, cells might reduce iron uptake to avoid the toxic effects of free iron ions. To assess the role of the Smu995-Smu998 system in alleviation of the Δ*dpr* phenotypes, we used a nonpolar kanamycin resistance cassette to replace the *smu995* gene (Δ*995*) or the entire *smu995-smu998* operon (Δ*995-998*) in both UA159 and Δ*dpr* backgrounds. We also took advantage of the availability of mutant FeoABC ferrous (Fe^{2+}) iron transport system strains of UA159 (Δ*feoA* and Δ*feoB*) (18) to obtain Δ*dpr* Δ*feoA* and Δ*dpr* Δ*feoB* double mutant strains. In agreement with predictions based on the WGS results, deletion of *smu995* alone or the *smu995-smu998* operon in the Δ*dpr* strain restored its ability to grow under aerobic conditions (Fig. 5A) and reversed the high sensitivity of the Δ*dpr* strain to H_2O_2 in a disc diffusion assay (Fig. 5B). On the other hand, deletion of either *feoA* or *feoB* in the Δ*dpr* strain did not affect expression of Δ*dpr* phenotypes (Fig. 5A and B). To estimate the relative availability of free iron within the different strains, we again resorted to the Fe-dependent antibiotic streptonigrin. Inactivation of *smu995-smu998* but not of *feoB* alleviated the increased sensitivity of the Δ*dpr* strain to streptonigrin (Fig. 5C). In fact, the Δ*dpr* Δ*995* and Δ*dpr* Δ*995-998* double mutant strains were significantly less sensitive to streptonigrin than the parent strain (Fig. 5C), which is consistent with diminished levels of intracellular free iron.

To determine whether loss of Dpr, either alone or coupled with the Δ*995* and Δ*feoB* mutations, affected intracellular iron content, we used inductively coupled plasma-optical emission spectrometry (ICP-OES) analyses to quantify the total iron content in the UA159, Δ*dpr*, Δ*dpr* Δ*995*, and Δ*dpr* Δ*feoB* strains grown under 5% CO_2 conditions. The total iron contents of the UA159 and Δ*dpr* strains were nearly identical, whereas both the Δ*dpr* Δ*995* and Δ*dpr* Δ*feoB* strains trended toward reductions in iron content compared to that of the parent and Δ*dpr* strains, though the differences were not significant (Fig. 5D). Interestingly, the transcriptional regulator Spx appears to govern transcription of both the *smu995-smu998* and *feoABC* operons. Recently, we performed transcriptome sequencing (RNA-Seq) analysis to study the H_2O_2 stress regulon as it relates to Spx regulation in *S. mutans* (26). When exposed to a subinhibitory concentration of H_2O_2, transcription of the *smu995-smu998* operon was higher in Δ*spxA1* and Δ*spxA1* Δ*spxA2* mutant strains than in the parent strain. During the stress exposure, the expression levels of *feoA* and *feoB* mirrored this trend, with increased expression in the Δ*spx* mutant strains compared to UA159. These gene expression trends indicate that Spx proteins serve as important regulators of iron transport systems in *S. mutans*.

Characterization of strains lacking *smu995-smu998*, *feoABC*, and *sloABC* reveals that the three systems contribute to iron uptake in *S. mutans*. The WGS analysis of

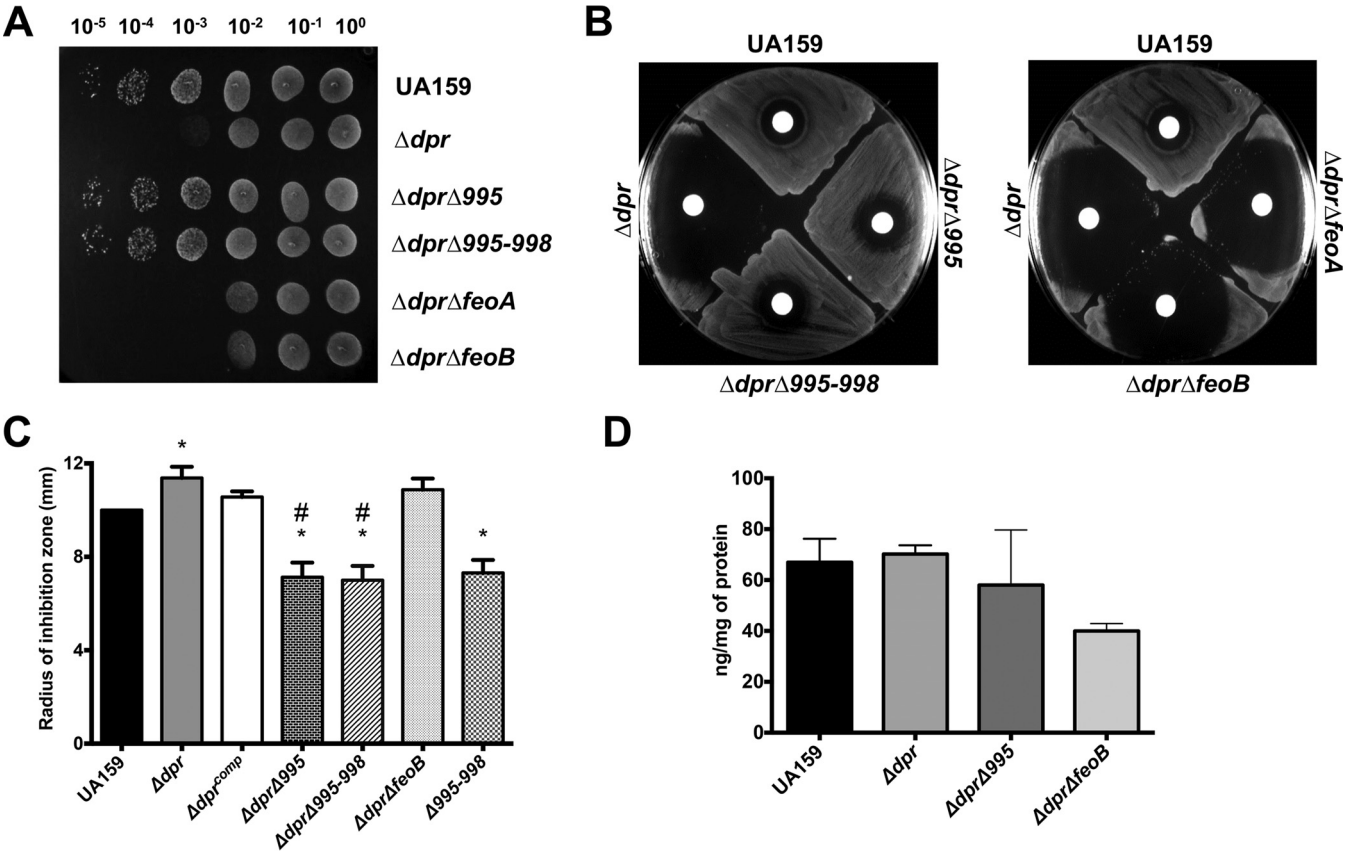

FIG 5 Inactivation of *smu995-smu998* but not of *feoAB* compensates for the loss of Dpr. (A) Tenfold serial dilutions of mid-exponential-phase cultures of the *S. mutans* UA159, Δ*dpr*, Δ*dpr* Δ*smu995*, Δ*dpr* Δ*smu995-smu998*, Δ*dpr* Δ*feoA*, and Δ*dpr* Δ*feoB* strains were spotted on BHI agar and incubated in 5% CO_2 for 24 h. (B and C) Early-logarithmic-phase cultures of *S. mutans* strains were swabbed onto a BHI agar plate, upon which filter paper discs saturated with H_2O_2 (B) or streptonigrin (C) were placed on top of the agar layer. Growth inhibition was observed after 24 h of incubation in 5% CO_2. (D) Total iron quantification of mid-logarithmic-phase cultures of *S. mutans* strains by ICP-OES. Total iron content was normalized to total protein content from the cell lysates. *, statistical significance compared to UA159 ($P < 0.05$, one-way ANOVA); #, statistical significance compared to the Δ*dpr* strain ($P < 0.01$, one-way ANOVA).

the Δ*dpr* revertants and phenotypic characterizations of double Δ*dpr* mutant strains (Δ*dpr* Δ*995*, Δ*dpr* Δ*995-998*, Δ*dpr* Δ*feoA*, and Δ*dpr* Δ*feoB*) suggested that the Smu995-Smu998 operon may be the major iron acquisition system of *S. mutans*. However, quantification of the total iron content of double mutant strains indicated that the FeoABC system may be more relevant to iron acquisition than Smu995-Smu998 (Fig. 5D). However, in this case, the Δ*dpr* background may be a confounding factor, as the Smu995-Smu998 and FeoABC systems could be responding differently to increases in intracellular free iron. In an attempt to identify the primary transport system responsible for iron uptake, we subjected strains lacking *smu995-smu998* (Δ*995-998*) or *feoABC* (Δ*feoB*) to streptonigrin sensitivity and ICP-OES analyses. We also included a strain lacking the *sloC* gene (Δ*sloC*) of the *sloABC* operon that was available in the lab as part of another project. Although SloABC, an ABC-type transporter, has been characterized as the major manganese transporter of *S. mutans*, this system is also known to participate in iron transport (27). In addition, we generated a double mutant strain lacking both *smu995-smu998* and *feoABC* (Δ*995-998* Δ*feoB*) as well as a triple mutant strain lacking all three transporters (Δ*sloC* Δ*995-998* Δ*feoB*). Among the single mutant strains, only the Δ*995-998* strain showed a small but significant increase in tolerance to streptonigrin in a disc diffusion assay (Fig. 6A) ($P < 0.05$), which agrees well with the results obtained with the Δ*dpr* double mutants (Fig. 5C). Most importantly, the double (Δ*995* Δ*feoB*) and triple (Δ*sloC* Δ*995* Δ*feoB*) mutant strains showed very high tolerance to streptonigrin, initially demonstrating no detectable growth inhibition at the concentration (0.05 μg μl^{-1}) routinely used to inhibit growth of the parent strain

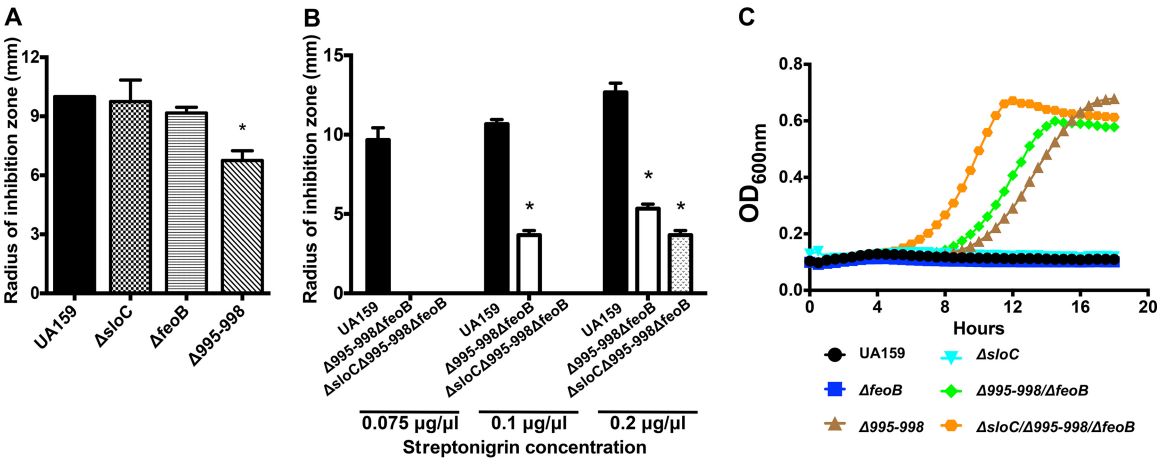

FIG 6 Characterization of the tolerance of *S. mutans* to the iron-dependent antibiotic streptonigrin following disruption of iron transport systems. (A and B) Measurement of zones of growth inhibition of early-logarithmic-phase cultures of the *S. mutans* UA159, Δ*sloC*, Δ*feoB*, and Δ*smu995-smu998* strains (A) and the UA159, Δ*995-998* Δ*feoB*, and Δ*sloC* Δ*995-998* Δ*feoB* strains (B) incubated in the presence of filter paper discs soaked with streptonigrin for 24 h. A lack of bars in panel B indicates that no growth inhibition was observed. (C) *S. mutans* UA159 and the panel of iron transport mutant strains were grown in BHI medium supplemented with 1 μg ml^{-1} of streptonigrin. Cells were grown to an OD_{600} of 0.5 in BHI and then diluted 1:40 into BHI containing streptonigrin. Growth was monitored using a BioScreen growth reader. *, statistical significance compared to UA159 ($P < 0.05$, one-way ANOVA).

(Fig. 6B). By increasing the concentration of streptonigrin to which the strains were exposed, we were able to obtain the first evidence that the three systems are involved in iron transport, with the double mutant showing some sensitivity at 0.1 μg μl^{-1} and the triple mutant showing growth inhibition only at the highest concentration (0.2 μg μl^{-1}) of streptonigrin tested (Fig. 6B). Next, we tested the abilities of the different iron transport mutant strains to grow in brain heart infusion (BHI) medium supplemented with 1 μg ml^{-1} streptonigrin. We observed that disruption of iron transport genes contributed to an enhanced ability to grow in the presence of streptonigrin, with the Δ*sloC* Δ*995-998* Δ*feoB* triple mutant strain demonstrating the greatest resistance to streptonigrin, followed by the Δ*995-998* Δ*feoB* double and Δ*995-998* single mutant strains (Fig. 6C). To further demonstrate the importance of iron in streptonigrin sensitivity, we also tested the ability of the Δ*995-998* and Δ*sloC* Δ*995-998* Δ*feoB* mutant strains to grow in the presence of streptonigrin in broth using the chemically defined medium FMC, replete with or depleted of iron. While growth in iron-replete medium showed that the parent strain was incrementally more sensitive to increased doses of streptonigrin, the strain became completely resistant to high concentrations of streptonigrin when iron was depleted from the growth medium (see Fig. S2 in the supplemental material). As observed in BHI plates, the Δ*995-998* single mutant strain and the Δ*sloC* Δ*995-998* Δ*feoB* triple mutant strain were highly tolerant to streptonigrin regardless of the iron concentration present in the growth medium (Fig. S2).

Next, we used ICP-OES to quantify the total iron content in the different iron transport mutants. Interestingly, all single mutant strains showed an approximately 30% reduction in total iron content, further indicating that the three transporters participate in iron acquisition (Fig. 7A). Unexpectedly, the iron contents of both double and triple mutant strains were similar to the iron content found in the single mutant strains, suggesting that *S. mutans* might have additional iron uptake mechanisms. To shed additional light onto the specific role of each transport system, we used real-time quantitative PCR (qRT-PCR) to explore the transcriptional responses of *feoB*, *sloC*, and *smu998* after cells of the parent strain were shifted from an anaerobic to an aerobic (via shaking growth) environment. A shift from anaerobic growth to vigorous shaking resulted in diminished relative transcription levels for *sloC* and *feoB* but not for *smu998* (Fig. 7B).

Concluding remarks. In the present study, we showed that the *S. mutans* Dpr accumulates during oxidative stress in an Spx-dependent manner, and we highlighted

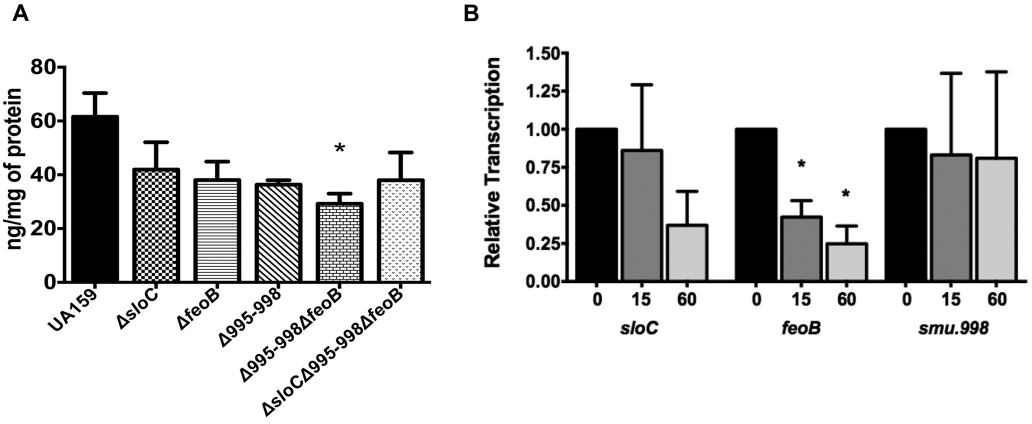

FIG 7 Characterization of total iron content and of expression levels of iron transport genes in response to stress. (A) The total cellular iron content of BHI-grown, mid-exponential-phase cultures of *S. mutans* UA159 and of strains bearing mutations in iron transport genes was determined by ICP-OES analysis. (B) Transcriptional profile of iron transport genes in *S. mutans* UA159. Cultures were grown in an anaerobic atmosphere to an OD_{600} of 0.4 (T_0) and then exposed to shaking (200 rpm) for 15 or 60 min. Bars represent the relative copy number detected for each gene compared to that at T_0. *, statistical significance compared to UA159 (A) or to T_0 for each gene (B) ($P < 0.05$, one-way ANOVA).

the central role of Dpr in oxidative stress and iron homeostasis. Although iron is an essential micronutrient, its involvement in Fenton chemistry and resulting production of highly damaging hydroxyl radicals means that the presence of intracellular free iron must be carefully controlled. Thus, without Dpr, the cell is presented with a unique challenge whereby it must acquire iron from the external environment in order to support enzymatic function, while simultaneously avoiding any excess in iron that, if not chelated by Dpr, can rapidly undergo Fenton chemistry. A common alternative used by Gram-positive bacteria such as *S. mutans* to avoid iron toxicity is to reduce their intracellular iron content (by either slowing import or increasing export) while bringing in millimolar concentrations of manganese that can be used to replace iron as an enzymatic cofactor (28). While the genome sequencing of Δ*dpr* revertants and subsequent inactivation of the Smu995-Smu998 system confirmed the power of next-generation sequencing to uncover genetic interactions by revealing the intimate linkage of Dpr with Smu995-Smu998, our initial characterization of the iron transport mutants only opens the door for a more thorough characterization of the mechanisms coordinating iron acquisition in *S. mutans*. Taken together, our results indicate that the *smu995-smu998* operon encodes a novel iron transport system of *S. mutans* that, along with FeoABC and SloABC, participates in iron acquisition. One common mechanism used by bacteria to acquire iron is via production of siderophores, low-molecular-weight organic molecules that are secreted to chelate iron from the environment and are brought back into the cells using surface-associated siderophore-iron receptors. Streptococci, however, are not known to synthesize siderophores (29), and a survey of the *S. mutans* genome does not reveal the presence of siderophore-encoding genes (27, 30). Interestingly, both GAS and GBS carry siderophore-iron transport genes that appear to mediate transport of siderophores produced by other bacteria, a mechanism known as siderophore piracy (22, 23). Genes of the *smu995-smu998* operon share low levels of homology with the siderophore-iron transport genes of GAS and GBS, and the *in vitro* characterization of strains lacking *smu995* or the entire *smu995-smu998* operon suggests that the Smu995-Smu998 system plays a role in iron transport even in the absence of siderophores. Previously, it had been proposed that iron import in *S. mutans* occurs mainly via the transport of Fe^{2+} iron, rather than Fe^{3+} iron, which is poorly soluble (30). At this point, it is unclear whether the Smu995-Smu998 system is involved in transporting Fe^{2+} or Fe^{3+} ions or whether it mediates iron uptake via siderophores. Finally, total iron quantifications of a triple mutant strain lacking the FeoABC, SloABC, and Smu995-Smu998 transporters strongly indicates that *S. mutans* possesses an additional, yet-to-be-identified iron transporter(s). Given the importance of iron for

TABLE 2 Bacterial strains and plasmids used in this study

Strain or plasmid	Relevant characteristics or application	Source or reference
Strains		
S. mutans		
UA159	Wild type	Laboratory stock
Δ*dpr* mutant	*dpr*::Erm	18
Δ*dpr*^{comp} mutant	Complementation of *dpr*	This study
Δ*spxA1* mutant	*spxA1*::Spec	35
Δ*spxA2* mutant	*spxA2*::Erm	35
Δ*spxA1* Δ*spxA2* mutant	*spxA1*::Spec *spxA2*::Erm	35
Δ*dpr* Δ*feoA* mutant	*dpr*::Erm *feoA*::Kan	This study
Δ*dpr* Δ*feoB* mutant	*dpr*::Erm *feoB*::Kan	This study
Δ*dpr* Δ*995* mutant	*dpr*::Erm *smu995*::Kan	This study
Δ*dpr* Δ*995-998* mutant	*dpr*::Erm *smu995-998*::Kan	This study
Δ*995-998* mutant	*smu995-998*::Kan	This study
Δ*feoB* mutant	*feoB*::Kan	18
Δ*sloC* mutant	*sloC*::Spec	This study
Δ*feo B*Δ*995-998* mutant	*feoB*::markerless *995-998*::Kan	This study
Δ*sloC* Δ*feoB* Δ*995-998* mutant	*sloC*::Spec *feoB*::markerless *995-998*::Kan	This study
E. coli		
DH10B	Cloning host	Laboratory stock
BL21(λDE3)	Protein expression host	Laboratory stock
Plasmids		
pMC340B	*S. mutans* integration vector	32
pET21-a(+)	His-tagged protein expression	Millipore Sigma

bacterial virulence, studies are in progress to further elucidate the mechanisms utilized by *S. mutans* to acquire and maintain iron homeostasis.

MATERIALS AND METHODS

Bacterial strains and growth conditions. The bacterial strains used in this study are listed in Table 2. The wild-type *S. mutans* UA159 strain and its derivatives were routinely grown in brain heart infusion (BHI) medium at 37°C in a 5% CO_2 atmosphere or under anaerobic conditions. All phenotypic characterization of strains lacking the *dpr* gene used cultures obtained from a freshly plated frozen stock of the Δ*dpr* strain grown under anaerobiosis (or on plates supplemented with catalase in a 5% CO_2 atmosphere) that consistently gave rise only to colonies that maintained high levels of sensitivity to growth in air or in the presence of H_2O_2. To assess the ability of *S. mutans* strains to grow in BHI or chemically defined FMC medium, BHI overnight cultures were diluted 1:20 into the appropriate medium and allowed to reach mid-exponential growth phase (optical density at 600 nm [OD_{600}] = 0.5). The cultures were then diluted 1:100 into fresh BHI or FMC medium in a microplate topped with a sterile mineral oil overlay to protect against excess oxidative stress. Growth at 37°C was monitored using the BioScreen growth reader (Oy Growth Curves). *Escherichia coli* strains were grown in Luria broth at 37°C for plasmid construction and propagation. When required for selective growth of strains, antibiotics were added to the growth medium as appropriate: kanamycin (1,000 μg ml^{-1} for *S. mutans* or 100 μg ml^{-1} for *E. coli*) or ampicillin (100 μg ml^{-1} for *E. coli*).

To determine Dpr levels under different growth conditions, *S. mutans* UA159 and Δ*spx* strains were grown in 5% CO_2 to an OD_{600} of 0.4 (T_0), and the culture was split in three parts, with one aliquot remaining in the 5% CO_2 incubator, another aliquot transferred to a 37°C shaker set to 200 rpm, and the third aliquot kept in 5% CO_2 but treated with 0.5 mM H_2O_2 for selected periods of time. To determine transcription levels of selected iron transport genes, *S. mutans* UA159 was grown anaerobically in BHI to an OD_{600} of 0.4. The culture was split in three parts; one was harvested immediately (T_0), and the other two were transferred to a 37°C shaker set to 200 rpm for harvesting after 15 or 60 min. Cells were harvested by centrifugation, resuspended in 1 ml RNAprotect bacterial reagent (Qiagen), and incubated at room temperature for 5 min. After an additional round of centrifugation, the supernatant was discarded, and cell pellets were stored at −80°C until use.

Construction of mutant and complemented strains. The *S. mutans* strains lacking the *smu995* or *sloC* gene or the entire *smu995-smu998* operon were constructed using a PCR ligation mutagenesis approach (31). Briefly, PCR fragments flanking the desired region to be deleted were ligated to a nonpolar kanamycin cassette (NP-Km^r) and the ligation mix used to transform *S. mutans* UA159. Double mutants were obtained by amplifying the mutated *dpr* region of the previously constructed Δ*dpr* strain (18) and then using this PCR product to transform the newly generated single mutant strains or the already available Δ*feoB* strain (18). Mutant strains were isolated on BHI plates supplemented with the appropriate antibiotic(s), and the deletions were confirmed by PCR sequencing of the insertion site and flanking region. Complementation of the Δ*dpr* strain was achieved by cloning the *dpr* gene into the *S. mutans* integration vector pMC340B (32). Briefly, the *dpr* coding sequence was amplified by PCR and

TABLE 3 Primers used in this study

Primer	Sequence (5′→3′)[a]	Application
dpr comp 5′KpnI	TTCGTTAAAGGGTACCAAATAATTGCT	*dpr* complementation
dpr comp 3′KpnI	GACTTCCTATCTGGTACCACTTATAAACC	
Dpr 5′NdeI	GAATATTTTTTAAGGAGGAATTCATATGACGAATAC	Dpr overexpression in *E. coli*
Dpr 3′XhoI	CTATCTTCACACTCGAGTAAACCGGGAG	
dpr Arm1 Forward	CAATCAGCCAGTCGGG	Construction of double Δ*dpr* mutants
dpr Arm2 Reverse	GCTGAAGCCACTGTTTC	
sloC 5′Arm1	GATCACGTTCTGCTTTTG	*sloC* deletion
sloC 3′Arm1 SphI	GTAATAATAAGCTTAGCATGCTCATTAG	
sloC 5′Arm2 SphI	GGTTGTTTCGCATGCTTCTCTTAAG	
sloC 3′Arm2	GATGCTGTTCCATATAC	
995 5′Arm1	CGAACCATGATTGTTGGTATTCCC	*smu995* deletion
995 3′Arm1 BamHI	CCAGCACTGGATCCGTGAGTAC	
995 5′Arm2 BamHI	CTATAGCTGGATCCGGAGAAG	
995 3′Arm2	CGCCACTTAATTCATCAAGAAAGCG	
995-998 5′Arm1	CGAACCATGATTGTTGGTATTCCC	*smu995-smu998* operon deletion
995-998 3′Arm1 BamHI	CCAGCACTGGATCCGTGAGTAC	
995-998 5′Arm2 BamHI	GGTAAAAATTGGATCCTTAATACAGGTGG	
995-998 3′Arm2	GCATTTTGCTCCTTCTTGAATCAGG	
sloC RT Fwd	CAGTGAGCGATAGTGTTAAGAC	*sloC* qRT-PCR
sloC RT Rev	CTCTTGTTTTTAGGATCTTTTTCAGATAG	
feoB RT Fwd	GGCTTATCAGATGGGAGTGC	*feoB* qRT-PCR
feoB RT Rev	GCAATCGCTGCTTCAAATTTGG	
smu998 RT Fwd	GAGCAACAATTGGTCAGGATGC	*smu998* qRT-PCR
smu998 RT Rev	GCTTTGGTTGTTCTAATACCACCTG	

[a]Underlining indicates restriction endonuclease recognition sites.

cloned into pMC340B to yield plasmid pMC340B-dpr. The plasmid was isolated in *E. coli* DH10B and used to transform the *S. mutans* Δ*dpr* strain for integration at the *mtl* locus. Primers used in this study are listed in Table 3.

Stress survival assays. To test sensitivity to H_2O_2 (Sigma-Aldrich) or streptonigrin (Sigma-Aldrich) in disc diffusion assays, a uniform layer of exponentially grown cells was spread onto agar plates using a sterile swab. Then, Whatman filter paper discs (6-mm diameter) saturated with 20 μl of 0.5% H_2O_2 solution or 0.05 μg μl^{-1} streptonigrin (unless a different concentration is mentioned) were placed on the agar. The radius of the zone of growth inhibition was measured after 24 h of incubation at 37°C in 5% CO_2 or under anaerobic conditions. To test sensitivity to ferrous iron ($FeSO_4$), exponentially grown cells were diluted 1:100 into plain BHI or BHI supplemented with 5 mM $FeSO_4$. The cultures were incubated for 24 h at 37°C in 5% CO_2, at which point 10-fold serial dilutions were prepared and plated for CFU enumeration.

WGS. *S. mutans* UA159 and three Δ*dpr* colony isolates were selected for whole-genome sequencing (WGS). The Δ*dpr* isolates were chosen to represent all combinations of phenotypes routinely observed for this strain, which included different morphologies (rough or smooth) demonstrating either sensitivity or resistance to oxidative stress. Upon confirmation that the stress phenotype was stable after multiple passages, 3 ml of cultures grown overnight in BHI under 5% CO_2 was harvested by centrifugation at 4°C for 10 min at 4,000 rpm, and the chromosomal DNA was isolated using the Qiagen DNeasy blood and tissue kit following the manufacturer's instructions for isolation of Gram-positive bacterial DNA, which included the addition of 25 U mutanolysin and 400 μg RNase A per sample during the pretreatment step. The WGS was performed at the University of Rochester Genomics Research Center (UR-GRC) using the Illumina MiSeq platform. Sequence reads were cleaned using Trimmomatic-0.32 before mapping to the UA159 genome using SHRiMP2.2.3. The genome sequences of the Δ*dpr* isolates were compared to that of UA159 to search for SNPs using SAMtools-1.2 and BCFtools-1.0.

Purification of recombinant Dpr and antibody generation. To express and purify Dpr, the promoter and coding region of the *dpr* gene were amplified from *S. mutans* UA159 using primers listed in Table 3. The amplified fragment and the expression vector pET-21a(+) (Millipore Sigma) were digested with NdeI and XhoI, ligated, and transformed by electroporation into *E. coli* BL21(λDE3). An isolate harboring the pET21a-rDpr plasmid was grown in LB containing ampicillin to an OD_{600} of 0.5, and expression of the His-tagged fusion protein was induced by treatment with 0.5 mM isopropyl-β-D-thiogalactopyranoside (IPTG) for 4 h. The recombinant protein was purified using the Ni-nitrilotriacetic acid (NTA) protein purification kit (Qiagen) according to the supplier's instructions. For generation of anti-rDpr polyclonal antibodies, adult rabbits were immunized with 1 mg of rDpr with Freund's adjuvant intravenously at days 1, 21, and 42 at Lampire Biological Laboratories (Pipersville, PA). After 50 days, the animals were bled, the titer of polyclonal antibodies in the serum against Dpr was determined by enzyme-linked immunosorbent assay, and the antibody specificity was confirmed by Western blotting using the wild-type and Δ*dpr* strains (data not shown).

Western blot analysis. Whole-cell protein lysates of *S. mutans* UA159, Δ*dpr*, or Δ*spx* strains were obtained by homogenization in the presence of 0.1-mm glass beads using a bead beater (Biospec). For staining of iron-binding proteins, $Fe(NH_4)_2(SO_4)$ was added to the whole-cell protein lysates at a final

concentration of 1 mM and incubated on ice for 30 min. The protein extracts were resolved by 8% nondenaturing PAGE (native PAGE) and stained with Ferene-S solution (2% acetic acid containing 1 mM Ferene-S and 15 mM thioglycolic acid) for 30 min at room temperature (33). Duplicate gels were stained with Coomassie brilliant blue as a loading control. To detect Dpr levels in the different *S. mutans* strains, protein lysates were separated by 15% SDS-PAGE and transferred to a polyvinylidene fluoride (PVDF) membrane (Millipore). Dpr detection was performed using rabbit anti-rDpr polyclonal antibody diluted 1:1,000 in phosphate-buffered saline (PBS) containing 0.1% Tween 20 (PBS-T) and anti-rabbit horseradish peroxidase (HRP)-coupled antibody (Sigma-Aldrich) diluted 1:2,000 in PBS-T. Immune reactivity was visualized by the incubation of the blot with 3,3-diaminobenzidine (Sigma-Aldrich) substrate solution for horseradish peroxidase conjugates. Densitometry was performed with Bio-Rad ImageQuant software in three independent experiments.

ICP-OES analysis. The total metal content within bacterial cells was determined by inductively coupled plasma-optical emission spectrometry (ICP-OES) at the University of Florida Institute of Food and Agricultural Sciences (UF-IFAS) Analytical Services Laboratories. Briefly, cultures (250 ml) were grown to mid-exponential phase, harvested by centrifugation at 4°C for 15 min at 4,000 rpm, and washed twice in ice-cold PBS supplemented with 0.5 mM EDTA to chelate extracellular divalent cations. Then, bacterial pellets were resuspended in 2 ml 35% HNO_3 and digested at 90°C for 1 h in a high-density polyethylene scintillation vial (Fisher Scientific). Digested bacteria were diluted 1:10 in reagent-grade H_2O prior to ICP-OES metal analysis. The metal composition was quantified using a 5300DV ICP atomic emission spectrometer (PerkinElmer), and concentrations were determined by comparisons to a standard curve. Metal concentrations were normalized to total protein content determined by the bicinchoninic acid (BCA) assay.

RNA extraction and qRT-PCR. Total RNA was isolated from *S. mutans* using our standard protocols as described previously (34). Briefly, RNA was isolated from homogenized *S. mutans* cells by acid-phenol-chloroform extractions and treated with DNase I (Ambion) at 37°C for 30 min. The RNA was purified using the RNeasy minikit (Qiagen), including two additional on-column DNase treatments as recommended by the supplier. RNA concentrations were determined using a NanoDrop spectrophotometer (Thermo Fisher). For real-time quantitative PCR (qRT-PCR), cDNA templates were created from 1 μg of RNA using MultiScribe reverse transcriptase (Applied Biosystems). Reactions were carried out on a CFX96 RT system (Bio-Rad) using iTaq Universal SYBR green Supermix (Bio-Rad) and the primer sets listed in Table 3.

SUPPLEMENTAL MATERIAL

Supplemental material for this article may be found at https://doi.org/10.1128/JB.00062-18.

SUPPLEMENTAL FILE 1, PDF file, 0.8 MB.

ACKNOWLEDGMENTS

This study was supported by NIH-NIDCR RO1 award DE019783 to J.A.L. The authors from the University of Campinas were supported by CAPES (Coordenação de Aperfeiçoamento de Pessoal de Nível Superior) (6849-12-1) and FAPESP (Fundação de Amparo à Pesquisa do Estado de São Paulo) (2012/032278-3 and 2014/03816-4).

REFERENCES

1. Bowen WH, Koo H. 2011. Biology of *Streptococcus mutans*-derived glucosyltransferases: role in extracellular matrix formation of cariogenic biofilms. Caries Res 45:69–86. https://doi.org/10.1159/000324598.
2. Lemos JA, Burne RA. 2008. A model of efficiency: stress tolerance by *Streptococcus mutans*. Microbiology 154:3247–3255. https://doi.org/10.1099/mic.0.2008/023770-0.
3. Marquis RE. 1995. Oxygen metabolism, oxidative stress and acid-base physiology of dental plaque biofilms. J Ind Microbiol 15:198–207. https://doi.org/10.1007/BF01569826.
4. Giacaman RA, Torres S, Gomez Y, Munoz-Sandoval C, Kreth J. 2015. Correlation of *Streptococcus mutans* and *Streptococcus sanguinis* colonization and *ex vivo* hydrogen peroxide production in carious lesion-free and high caries adults. Arch Oral Biol 60:154–159. https://doi.org/10.1016/j.archoralbio.2014.09.007.
5. Kreth J, Zhang Y, Herzberg MC. 2008. Streptococcal antagonism in oral biofilms: *Streptococcus sanguinis* and *Streptococcus gordonii* interference with *Streptococcus mutans*. J Bacteriol 190:4632–4640. https://doi.org/10.1128/JB.00276-08.
6. Imlay JA. 2013. The molecular mechanisms and physiological consequences of oxidative stress: lessons from a model bacterium. Nat Rev Microbiol 11:443–454. https://doi.org/10.1038/nrmicro3032.
7. Harrison PM, Arosio P. 1996. The ferritins: molecular properties, iron storage function and cellular regulation. Biochim Biophys Acta 1275:161–203. https://doi.org/10.1016/0005-2728(96)00022-9.
8. Calhoun LN, Kwon YM. 2011. The ferritin-like protein Dps protects *Salmonella enterica* serotype *Enteritidis* from the Fenton-mediated killing mechanism of bactericidal antibiotics. Int J Antimicrob Agents 37:261–265. https://doi.org/10.1016/j.ijantimicag.2010.11.034.
9. Yamamoto Y, Fukui K, Koujin N, Ohya H, Kimura K, Kamio Y. 2004. Regulation of the intracellular free iron pool by Dpr provides oxygen tolerance to *Streptococcus mutans*. J Bacteriol 186:5997–6002. https://doi.org/10.1128/JB.186.18.5997-6002.2004.
10. Zhao G, Ceci P, Ilari A, Giangiacomo L, Laue TM, Chiancone E, Chasteen ND. 2002. Iron and hydrogen peroxide detoxification properties of DNA-binding protein from starved cells. A ferritin-like DNA-binding protein of *Escherichia coli*. J Biol Chem 277:27689–27696.
11. Martinez A, Kolter R. 1997. Protection of DNA during oxidative stress by the nonspecific DNA-binding protein Dps. J Bacteriol 179:5188–5194. https://doi.org/10.1128/jb.179.16.5188-5194.1997.
12. Hua CZ, Howard A, Malley R, Lu YJ. 2014. Effect of nonheme iron-containing ferritin Dpr in the stress response and virulence of pneumococci. Infect Immun 82:3939–3947. https://doi.org/10.1128/IAI.01829-14.
13. Tsou CC, Chiang-Ni C, Lin YS, Chuang WJ, Lin MT, Liu CC, Wu JJ. 2010. Oxidative stress and metal ions regulate a ferritin-like gene, *dpr*, in *Streptococcus pyogenes*. Int J Med Microbiol 300:259–264. https://doi.org/10.1016/j.ijmm.2009.09.002.
14. Yamamoto Y, Poole LB, Hantgan RR, Kamio Y. 2002. An iron-binding protein, Dpr, from *Streptococcus mutans* prevents iron-dependent hy-

droxyl radical formation *in vitro*. J Bacteriol 184:2931–2939. https://doi.org/10.1128/JB.184.11.2931-2939.2002.
15. Zhang T, Ding Y, Li T, Wan Y, Li W, Chen H, Zhou R. 2012. A Fur-like protein PerR regulates two oxidative stress response related operons *dpr* and *metQIN* in *Streptococcus suis*. BMC Microbiol 12:85. https://doi.org/10.1186/1471-2180-12-85.
16. Zhu L, Kreth J. 2012. The role of hydrogen peroxide in environmental adaptation of oral microbial communities. Oxid Med Cell Longev 2012:717843. https://doi.org/10.1155/2012/717843.
17. Yamamoto Y, Higuchi M, Poole LB, Kamio Y. 2000. Role of the *dpr* product in oxygen tolerance in *Streptococcus mutans*. J Bacteriol 182:3740–3747. https://doi.org/10.1128/JB.182.13.3740-3747.2000.
18. Galvao LC, Miller JH, Kajfasz JK, Scott-Anne K, Freires IA, Franco GC, Abranches J, Rosalen PL, Lemos JA. 2015. Transcriptional and phenotypic characterization of novel Spx-regulated genes in *Streptococcus mutans*. PLoS One 10:e0124969. https://doi.org/10.1371/journal.pone.0124969.
19. Fujishima K, Kawada-Matsuo M, Oogai Y, Tokuda M, Torii M, Komatsuzawa H. 2013. *dpr* and *sod* in *Streptococcus mutans* are involved in coexistence with *S. sanguinis*, and PerR is associated with resistance to H_2O_2. Appl Environ Microbiol 79:1436–1443. https://doi.org/10.1128/AEM.03306-12.
20. Yamamoto Y, Higuchi M, Poole LB, Kamio Y. 2000. Identification of a new gene responsible for the oxygen tolerance in aerobic life of *Streptococcus mutans*. Biosci Biotechnol Biochem 64:1106–1109. https://doi.org/10.1271/bbb.64.1106.
21. Yeowell HN, White JR. 1982. Iron requirement in the bactericidal mechanism of streptonigrin. Antimicrob Agents Chemother 22:961–968. https://doi.org/10.1128/AAC.22.6.961.
22. Clancy A, Loar JW, Speziali CD, Oberg M, Heinrichs DE, Rubens CE. 2006. Evidence for siderophore-dependent iron acquisition in group B streptococcus. Mol Microbiol 59:707–721. https://doi.org/10.1111/j.1365-2958.2005.04974.x.
23. Hanks TS, Liu M, McClure MJ, Lei B. 2005. ABC transporter FtsABCD of *Streptococcus pyogenes* mediates uptake of ferric ferrichrome. BMC Microbiol 5:62. https://doi.org/10.1186/1471-2180-5-62.
24. Hung KW, Tsai JY, Juan TH, Hsu YL, Hsiao CD, Huang TH. 2012. Crystal structure of the *Klebsiella pneumoniae* NFeoB/FeoC complex and roles of FeoC in regulation of Fe^{2+} transport by the bacterial Feo system. J Bacteriol 194:6518–6526. https://doi.org/10.1128/JB.01228-12.
25. Seyedmohammad S, Fuentealba NA, Marriott RA, Goetze TA, Edwardson JM, Barrera NP, Venter H. 2016. Structural model of FeoB, the iron transporter from *Pseudomonas aeruginosa*, predicts a cysteine lined, GTP-gated pore. Biosci Rep 36:e00322. https://doi.org/10.1042/BSR20160046.
26. Kajfasz JK, Ganguly T, Hardin EL, Abranches J, Lemos JA. 2017. Transcriptome responses of *Streptococcus mutans* to peroxide stress: identification of novel antioxidant pathways regulated by Spx. Sci Rep 7:16018. https://doi.org/10.1038/s41598-017-16367-5.
27. Paik S, Brown A, Munro CL, Cornelissen CN, Kitten T. 2003. The *sloABCR* operon of *Streptococcus mutans* encodes an Mn and Fe transport system required for endocarditis virulence and its Mn-dependent repressor. J Bacteriol 185:5967–5975. https://doi.org/10.1128/JB.185.20.5967-5975.2003.
28. Eijkelkamp BA, McDevitt CA, Kitten T. 2015. Manganese uptake and streptococcal virulence. Biometals 28:491–508. https://doi.org/10.1007/s10534-015-9826-z.
29. Turner AG, Ong CY, Walker MJ, Djoko KY, McEwan AG. 2017. Transition metal homeostasis in *Streptococcus pyogenes* and *Streptococcus pneumoniae*. Adv Microb Physiol 70:123–191. https://doi.org/10.1016/bs.ampbs.2017.01.002.
30. Evans SL, Arceneaux JE, Byers BR, Martin ME, Aranha H. 1986. Ferrous iron transport in *Streptococcus mutans*. J Bacteriol 168:1096–1099. https://doi.org/10.1128/jb.168.3.1096-1099.1986.
31. Lau PC, Sung CK, Lee JH, Morrison DA, Cvitkovitch DG. 2002. PCR ligation mutagenesis in transformable streptococci: application and efficiency. J Microbiol Methods 49:193–205. https://doi.org/10.1016/S0167-7012(01)00369-4.
32. Chen PM, Chen YY, Yu SL, Sher S, Lai CH, Chia JS. 2010. Role of GlnR in acid-mediated repression of genes encoding proteins involved in glutamine and glutamate metabolism in *Streptococcus mutans*. Appl Environ Microbiol 76:2478–2486. https://doi.org/10.1128/AEM.02622-09.
33. Tsou CC, Chiang-Ni C, Lin YS, Chuang WJ, Lin MT, Liu CC, Wu JJ. 2008. An iron-binding protein, Dpr, decreases hydrogen peroxide stress and protects Streptococcus pyogenes against multiple stresses. Infect Immun 76:4038–4045. https://doi.org/10.1128/IAI.00477-08.
34. Abranches J, Candella MM, Wen ZT, Baker HV, Burne RA. 2006. Different roles of EIIABMan and EIIGlc in regulation of energy metabolism, biofilm development, and competence in *Streptococcus mutans*. J Bacteriol 188:3748–3756. https://doi.org/10.1128/JB.00169-06.
35. Kajfasz JK, Martinez AR, Rivera-Ramos I, Abranches J, Koo H, Quivey RG, Jr, Lemos JA. 2009. Role of Clp proteins in expression of virulence properties of *Streptococcus mutans*. J Bacteriol 191:2060–2068. https://doi.org/10.1128/JB.01609-08.